Storm 860 and the ImageQuant TL software version 2003.02 (GE Healthcare).

*In vitro effect of SP on cAMP and $IP_3$ levels, proliferation, and phosphorylation of PKA and ERK1/2 of immortalized large cholangiocytes.* For the measurement of cAMP or $IP_3$ levels, large immortalized cholangiocytes were treated at room temperature for 5 (cAMP) (3, 15) or 10 ($IP_3$) (16) min with 0.2% bovine serum albumin (BSA) or SP ($10^{-9}$ M) before evaluation of the levels of these two molecules by RIA (2, 3, 15, 16). In other experiments, large cholangiocyte lines were treated at 37°C for 24, 48, and 72 h with 0.2% BSA or SP ($10^{-6}$ to $10^{-11}$ M) before evaluation of cell proliferation by CellTiter 96 Cell Proliferation Assay (Promega, Madison, WI) (16). In separate sets of experiments, large cholangiocytes were treated at 37°C for 48 h with 0.2% BSA (basal) or SP ($10^{-9}$ M) for 48 h in the absence or presence of preincubation with spantide (a specific NK-1R inhibitor, $10^{-6}$ M) (24), BAPTA/AM (5 μM) (16), or H89 (a PKA inhibitor, 30 μM) (22) before evaluation of proliferation by CellTiter 96 Cell Proliferation Assay. Absorbance was measured at 490 nm on a microplate spectrophotometer (Molecular Devices, Sunnyvale, CA). Data were expressed as the fold change of treated cells compared with BSA-treated cells. Also, large cholangiocytes were stimulated with 0.2% BSA or SP ($10^{-9}$ M for 1, 2, and 6 h) before evaluation by immunoblots (19) of the proliferation (by PCNA) and the phosphorylation of PKA. The intensity of the bands was determined by scanning video densitometry (see above). Large cholangiocytes were also stimulated with 0.2% BSA or SP ($10^{-9}$ M for 1, 2, 3, 5, 7, 10, 20, 30, 60, and 90 min, 1, 2, and 6 h) before evaluation of ERK1/2 phosphorylation by immunoblots (19).

*Statistical analysis.* All data are expressed as means ± SE. Differences between groups were analyzed by the Student's unpaired *t*-test when two groups were analyzed and by ANOVA when more than two groups were analyzed, followed by an appropriate post hoc test.

## RESULTS

*Expression of NK-1R in liver sections and isolated and immortalized large cholangiocytes.* By semiquantitative immunohistochemistry, the expression of NK-1R was low in bile ducts from WT (red arrow) normal mice but increased in bile ducts from WT BDL mice (Fig. 1*A*; yellow arrows and Table 1). NK-1R was absent in bile ducts from normal and BDL NK-$1R^{-/-}$ mice (Fig. 1*A* and Table 1). These findings were confirmed by immunoblotting: the expression of NK-1R increased in large cholangiocytes from BDL WT mice compared with large cholangiocytes from normal WT mice (Fig. 1*B*); NK-1R was also expressed by small bile ducts in liver sections (not shown). By immunofluorescence, specific immunoreactivity for NK-1R in representative fields of large murine cholangiocyte lines (44) is shown in red; cell nuclei were stained with DAPI (blue) (Figs. 1*C*).

*Evaluation of serum levels of transaminases and bilirubin, lobular necrosis, inflammation, hepatocyte apoptosis and steatosis, and cholangiocyte proliferation and apoptosis.* Surprisingly, body weight was significantly lower in WT BDL mice compared with NK-$1R^{-/-}$ BDL mice (Table 1). In both normal and BDL NK-$1R^{-/-}$ mice there was a significant decrease in liver-to-body weight ratio (an index of liver growth including cholangiocytes) (4) compared with the corresponding WT mice

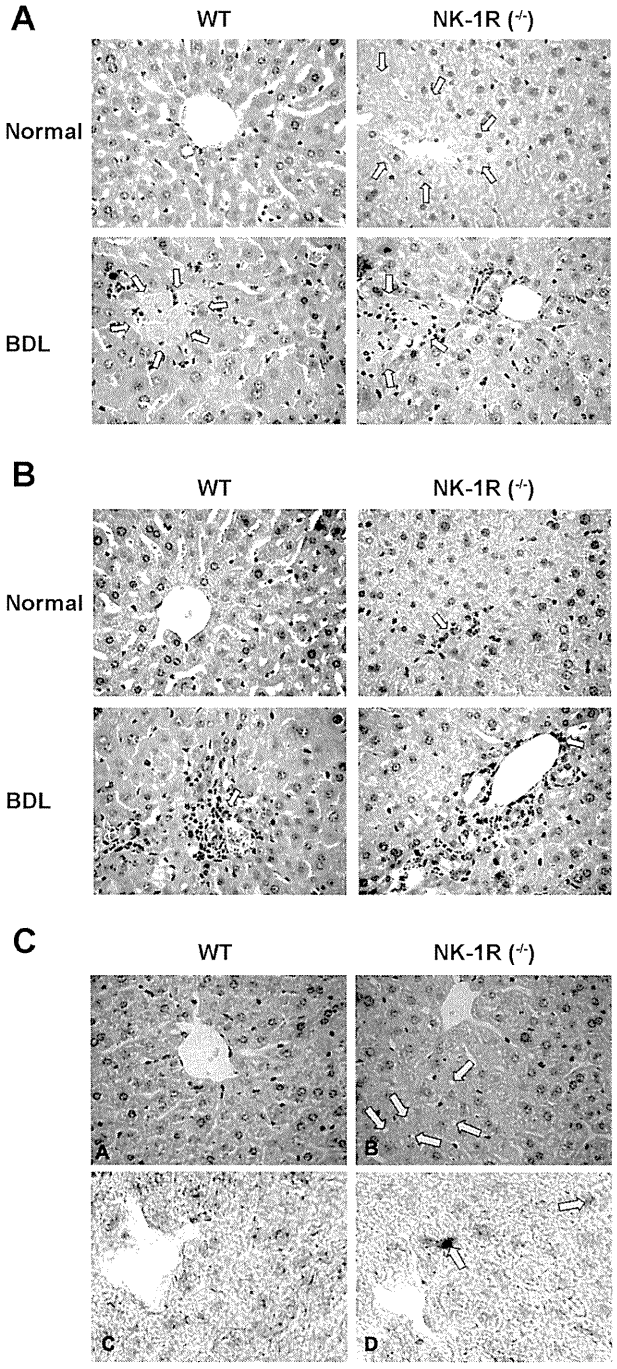


Fig. 2. Evaluation of necrosis (*A*), inflammatory infiltrates (by H&E staining) (*B*), and steatosis [by H&E staining (*CA* and *CB*) and oil red O staining (*CC* and *CD*)] in liver sections from the experimental groups of Table 1. In sections from normal NK-$1R^{-/-}$ mice, we observed some necrotic areas (yellow arrows; *A*) and inflammatory infiltrates (yellow arrow *B*) compared with normal WT mice. There was a decrease in necrotic areas in NK-$1R^{-/-}$ BDL mice compared with BDL WT mice. No marked difference in inflammatory infiltrate was observed between WT and NK-$1R^{-/-}$ BDL mice. By hematoxylin and eosin (H&E; *CA* and *CB*) and oil red O (*CC* and *CD*) staining, in NK-$1R^{-/-}$ normal mice, centrolobular liver parenchyma shows round-shaped areas (yellow arrows) evocative of steatosis (*CB*) and scattered red areas highlighted by oil red O stain method, a specific stain for neutral lipids (yellow arrows) (*CD*). WT normal mice samples show normal liver morphology without oil red O stain (*CA* and *CC*). (Light microscopy: *CA* and *CB*, H&E, original magnification ×20; *CC* and *CD*, oil red O staining in frozen liver sections, original magnification ×40).

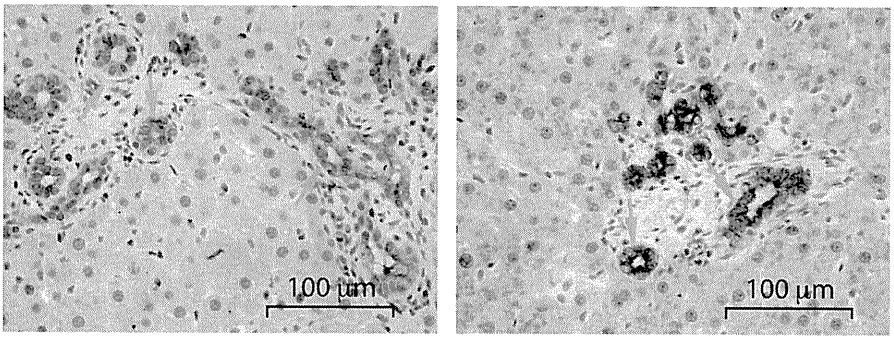


Fig. 3. Immunohistochemistry for CK-19 in liver sections from WT and NK-1R$^{-/-}$ BDL mice. There was a decrease in the number of large CK-19-positive cholangiocytes in liver sections from NK-1R$^{-/-}$ BDL mice compared with 7-day BDL WT mice (for semiquantitative data, see Table 4). Original magnification ×40.

(Table 1). In agreement with previous studies in rodents (4), the serum levels of transaminases (alanine aminotransferase and aspartate aminotransferase) and total bilirubin were higher in WT BDL mice compared with normal WT mice and decreased in NK-1R$^{-/-}$ BDL mice compared with WT BDL mice (Table 2). No difference in the serum levels of total bilirubin was observed between WT normal mice and NK-1R$^{-/-}$ normal mice (Table 2). Surprisingly, we observed a significant increase in the serum levels of transaminases in normal NK-1R$^{-/-}$ mice compared with WT normal mice (Table 2).

In liver sections from normal NK-1R$^{-/-}$ mice, we observe higher hepatocyte apoptosis (Table 3), some necrotic areas (yellow arrows, Fig. 2*A*) and inflammatory infiltrates (yellow arrow, Fig. 2*B*) compared with normal WT mice. There was a decrease in necrotic areas in NK-1R$^{-/-}$ BDL mice compared with BDL WT mice (see yellow arrows) (Fig. 2*A*). No marked difference in inflammatory infiltrate was observed between WT and NK-1R$^{-/-}$ BDL mice (see yellow arrow) (Fig. 2*B*). In NK-1R$^{-/-}$ normal mice, centrolobular liver parenchyma shows round-shaped areas (Fig. 2*C*) and red scattered spots by oil red O staining evocative of steatosis (Fig. 2*C*), whereas WT (Fig. 2*C*) and heterozygous (not shown) normal mice samples display normal liver morphology. All BDL liver sections do not present round-shaped areas evocative of steatosis (not shown). No significant differences in these parameters were seen between WT and NK-1R$^{-/-}$ normal mice (not shown). These histomorphological changes (Fig. 2, *A–C* and Table 3) likely explain the significant increase in the serum levels of transaminases observed in normal NK-1R$^{-/-}$ mice compared with WT normal mice. The number of PCNA-positive cholangiocytes was low and similar in both WT (0.4 ± 0.2) and NK-1R$^{-/-}$ (0.2 ± 0.2) normal mice. In NK-1R$^{-/-}$ BDL mice, there was a decrease in the number of PCNA-positive large cholangiocytes (17.4 ± 1.3) compared with WT BDL mice (12.0 ± 1.3). The number of CK-19-positive large cholangiocytes was similar among WT, heterozygous, and NK-1R$^{-/-}$ normal mice and increased following BDL in both WT and heterozygous BDL mice (Fig. 3 and Table 4). In NK-1R$^{-/-}$ BDL mice, there was a decrease in the number of CK-19-positive large cholangiocytes compared with WT BDL mice (Fig. 3 and Table 4). In heterozygous BDL mice, the number of CK-19-positive cholangiocytes was lower than that of BDL WT mice but higher than NK-1R$^{-/-}$ BDL mice (Table 4). In NK-1R$^{-/-}$ and heterozygous BDL mice, there was a concomitant increase in the number of TUNEL-positive large cholangiocytes compared with the degree of cholangiocyte apoptosis observed in the corresponding WT BDL mice (Table 4). No difference in cholangiocyte apoptosis was observed between WT and heterozygous normal mice and NK-1R$^{-/-}$ normal mice (Table 4). No significant gross postmortem or pathological changes were detected in the body cavities, integumentary, alimentary, respiratory, circulatory, nervous, urogenital, hematopoietic, and musculoskeletal systems of normal WT mice and NK-1R$^{-/-}$ normal mice (not shown).

*mRNA expression for collagen 1α and α-SMA.* No changes in the mRNA and protein expression of collagen 1α were observed in total liver samples from WT and NK-1R$^{-/-}$ normal mice (Fig. 4*A*). The expression of α-SMA decreased in total liver samples from normal NK-1R$^{-/-}$ mice compared with normal WT mice (Fig. 4*B*). The expression of collagen 1α and α-SMA increased in total liver samples from BDL WT mice compared with normal WT mice (Fig. 4, *A* and *B*). There was a decrease expression of collagen 1α and α-SMA mRNA expression in total liver samples from BDL NK-1R$^{-/-}$ mice compared with total liver samples from BDL WT mice (Fig. 4, *A* and *B*).

*Measurement of PCNA protein expression, and phosphorylation of cAMP-dependent PKA in isolated large cholangiocytes.* There was a decrease in PCNA expression in large cholangiocytes from NK-1R$^{-/-}$ BDL mice compared with large cholangiocytes from WT BDL mice (Fig. 5*A*). In large cholangiocytes from NK-1R$^{-/-}$ BDL mice there was a decrease in the phosphorylation of cAMP-dependent PKA compared with large cholangiocytes from WT BDL mice (Fig. 5*B*).

Table 4. *Evaluation of the number of CK-19 or TUNEL-positive large cholangiocytes*

| Groups | Number of CK-19-Positive Cholangiocytes | Number of Cholangiocytes Positive by TUNEL |
|---|---|---|
| WT normal mice | 17.2 ± 1.0 | ND |
| Heterozygous normal mice | 17.3 ± 1.1 | ND |
| NK-1R$^{-/-}$ normal mice | 17.1 ± 1.8 | 0.3 ± 0.1 |
| WT 7 BDL mice | 78.8 ± 4.3* | 1.2 ± 0.2 |
| Heterozygous BDL mice | 65.1 ± 2.0* | 4.2 ± 0.2 |
| NK-1R$^{-/-}$ BDL mice | 53.0 ± 2.6† | 6.6 ± 0.4† |

Data are means ± SE. *$P < 0.05$ vs. the corresponding value of normal WT mice. †$P < 0.05$ vs. the corresponding value of WT mice with BDL for 7 days.

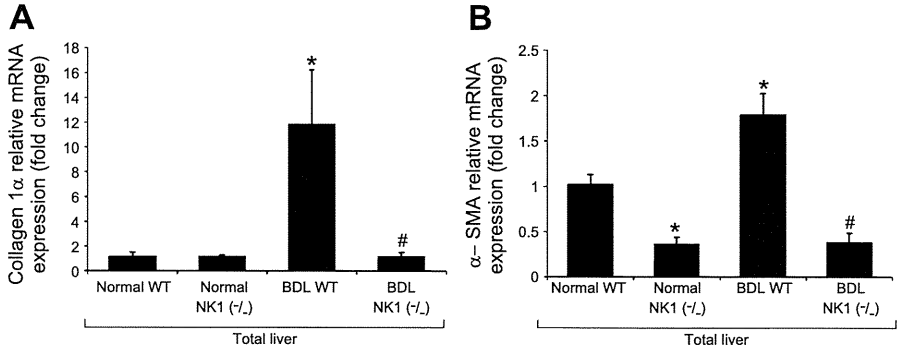


Fig. 4. Evaluation of the mRNA and protein expression of collagen 1α (*A*) and α-smooth muscle actin (α-SMA; *B*) in total liver tissue from WT and NK-1R$^{-/-}$ normal and BDL mice. No changes in the expression of collagen 1α were observed in total liver samples from normal WT and normal NK-1R$^{-/-}$ mice. The expression of α-SMA decreased in total liver samples from normal NK-1R$^{-/-}$ mice compared with normal WT mice. The expression of collagen 1α and α-SMA increased in total liver samples from BDL WT mice compared with normal WT mice. There was a decrease expression of collagen 1α and α-SMA mRNA expression in total liver samples from BDL NK-1R$^{-/-}$ mice compared with total liver samples from BDL WT mice. *$P < 0.05$ vs. the corresponding value of normal WT mice. #$P < 0.05$ vs. the corresponding value of WT BDL mice.

*In vitro effect of SP on cAMP and $IP_3$ levels, cholangiocyte proliferation, and phosphorylation of PKA and ERK1/2 of large cholangiocytes.* A marked increase in cAMP levels was observed with forskolin (an activator of adenylyl cyclase) (17), whereas secretin and SP induced a modest yet significant increase in cAMP levels in large cholangiocytes (Fig. 6*A*). The increase in cAMP levels observed with secretin in immortalized large cholangiocytes was similar to that observed in our previous studies (17). SP did not increase $IP_3$ levels of large cholangiocytes (Fig. 6*B*). By MTS assays, SP induced a similar and sustained (both at 48 and 72 h) increases in the proliferation of large cholangiocytes compared with controls (Fig. 7, *A* and *B*); no increase was seen at 24 h of treatment with SP (not shown). SP stimulation of large cholangiocyte growth was blocked by preincubation with spantide and H89 at 48 h and partly at 72 h (Fig. 7 *C* and *D*); BAPTA/AM did not block substance stimulation of large cholangiocyte proliferation (Fig. 7 *C* and *D*). Short-term treatment with SP increased PCNA protein expression and phosphorylation of PKA (but not ERK1/2, not shown) compared with controls (Fig. 8, *A* and *B*).

## DISCUSSION

Previous studies have demonstrated that *1*) circulating levels of the sensory neuropeptides CGRP, SP, and adrenomedullin are elevated in humans, and rodent models of cirrhosis and biliary hyperplasia (11, 23, 29, 40); and *2*) SP serum levels are elevated in cholestatic patients and BDL rats (42). Our study provides the first evidence regarding the role of the SP→NK-1R axis in sustaining the proliferation of large cholangiocytes by activation of cAMP signaling. We found an increase in the serum levels of transaminases in normal NK-1R$^{-/-}$ mice compared with WT normal mice. The serum levels of transaminases and total bilirubin were decreased in NK-1R$^{-/-}$ BDL mice compared with WT BDL mice. We demonstrated the presence of NK-1R in large cholangiocytes that was higher in BDL compared with normal rats. Knockdown of the NK-1R gene in BDL mice induces a decrease (~40%) in the number of large cholangiocytes (associated with enhanced biliary apoptosis) compared with BDL WT mice. There was decreased PCNA protein expression and phosphorylation of PKA in large cholangiocytes from NK-1R$^{-/-}$ BDL mice

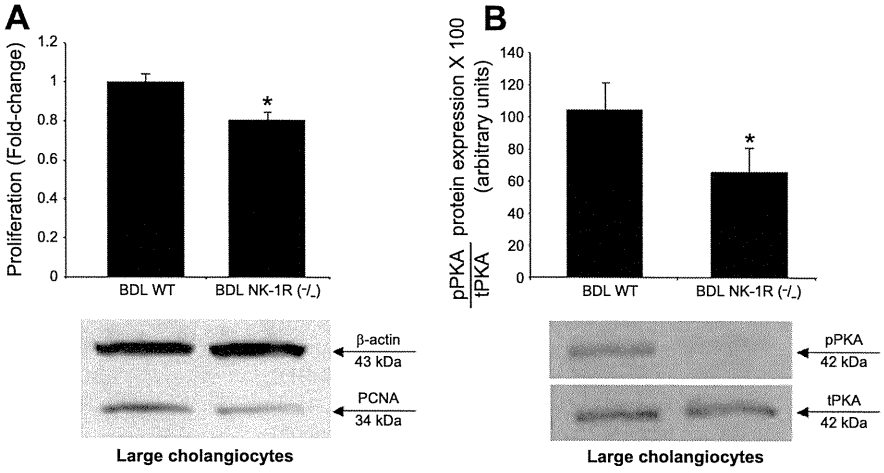


Fig. 5. Evaluation of PCNA expression and cAMP-dependent phosphorylation of PKA in large cholangiocytes from WT and NK-1R$^{-/-}$ BDL mice. There was decreased PCNA expression (*A*) and phosphorylation of PKA (*B*) in large cholangiocytes from NK-1R$^{-/-}$ BDL mice compared with large cholangiocytes from WT BDL mice. Data are means ± SE of 6 immunoblots derived from protein obtained from cumulative preparations of cholangiocytes. pPKA, phosphorylated PKA; tPKA, total PKA. *$P < 0.05$ vs. the corresponding value of BDL large cholangiocytes. *$P < 0.05$ vs. the corresponding value of BDL large cholangiocytes.

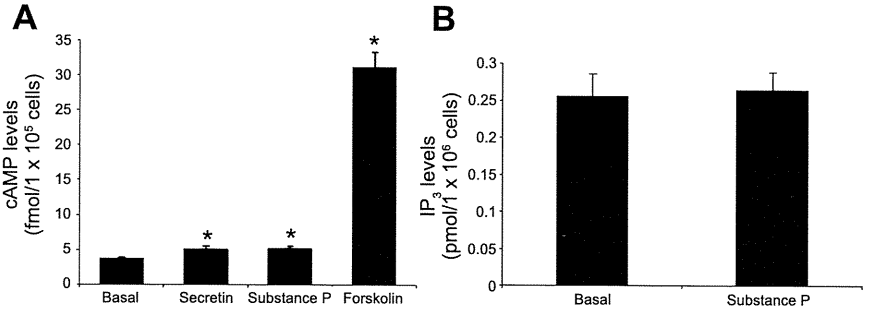


Fig. 6. In vitro effect of forskolin ($10^{-4}$ M), secretin (100 nM) and substance P (10 μM) on cAMP (*A*) and substance P (10 μM) on D-myo-inositol 1,4,5-trisphosphate ($IP_3$) levels (*B*) of large cholangiocytes. *A*: a massive increase in cAMP levels was observed with forskolin, whereas secretin and substance P induced a modest albeit significant increase in cAMP levels in large cholangiocytes. *B*: substance P did not increase $IP_3$ levels of large cholangiocytes. Substance P increased cAMP (*A*) but not $IP_3$ (*B*) levels of large cholangiocytes. Data are means ± SE of 6 values obtained from cumulative preparations of cholangiocytes. $*P < 0.05$ vs. the corresponding basal value of large cholangiocytes treated with 0.2% BSA (basal).

compared with controls. The expression of collagen 1α and α-SMA increased in total liver samples from BDL WT mice compared with normal WT mice and decreased in BDL NK-$1R^{-/-}$ mice compared with total liver samples from BDL WT mice. In vitro, SP increased cAMP levels, enhanced the phosphorylation of PKA but not ERK1/2, and induced a sustained increase in the proliferation of large cholangiocytes. Pharmacological targeting of NK-1R may be important in the inhibition of biliary proliferation in cholestatic liver disorders.

In support for the presence of NK-1R in liver, previous studies have demonstrated the presence of NK-1R in hepatocytes (9, 10). Although both small (not shown) and large cholangiocytes express NK-1R, we evaluated the role of the SP→NK-1R axis on the regulation of large cholangiocyte growth since large, but not small, cholangiocytes proliferate in response to BDL (3, 15, 31). Previous studies have emphasized the importance of cAMP/PKA/ERK1/2 signaling in the regulation of large biliary functions (8). For example, the stimulation of adenylyl cyclase by forskolin stimulates large cholangiocyte proliferation (17). Maintenance of cholangiocyte cAMP levels by administration of forskolin prevents the functional damage of bile ducts induced by vagotomy (30). Since *1*) small cholangiocytes (whose function is regulated by $IP_3/Ca^{2+}$) (16, 20) express NK-1R and *2*) SP exerts its cellular function by the activation of both cAMP and $IP_3/Ca^{2+}$ signaling (26, 36), studies aimed to evaluate the role of SR in small cholangiocyte functions are necessary. Also, further experiments aimed to evaluate the effects of SP on the phosphorylation of other MAPK isoforms such as JNK and p38 in large cholangiocytes are underway and part of another project.

In our NK-$1R^{-/-}$ BDL model, the extent of the reduction (~40%) of biliary mass is consistent with the concept that cholangiocyte proliferation is coordinately modulated by a number of stimulatory/inhibitory neuroendocrine factors (7). A similar reduction in biliary was observed in α-CGRP $BDL^{-/-}$ mice (23) since other sensory neuropeptides such as β-CGRP

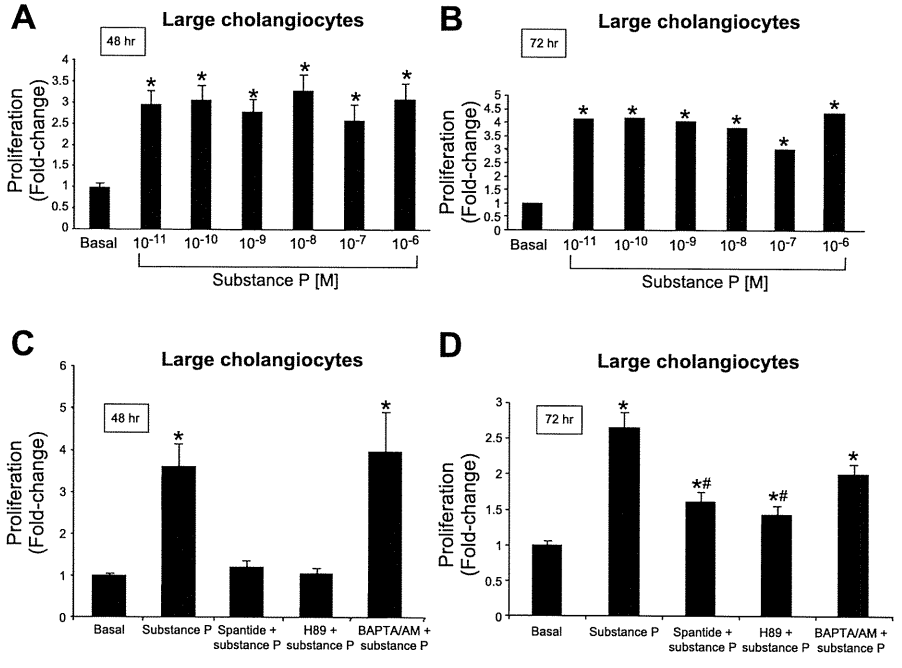


Fig. 7. *A* and *B*: by MTS assays, substance P induced a similar (at all the doses used) and sustained (24 and 72 h) increase in the proliferation of large cholangiocytes compared with BSA-treated cells. Data are means ± SE of 6 experiments. $*P < 0.05$ vs. the corresponding basal value of large cholangiocytes. *C* and *D*: effect of 0.2% BSA (basal) or substance P ($10^{-9}$ M) for 48 h in the absence or presence of preincubation with spantide (specific NK-1R inhibitor), H89 (PKA inhibitor), or BAPTA/AM (intracellular $Ca^{2+}$ chelator). Substance P stimulation of large cholangiocyte growth was blocked by preincubation with spantide and H89 but not BAPTA/AM. Data are means ± SE of 6 experiments. $*P < 0.05$ vs. the corresponding basal value of large cholangiocytes.

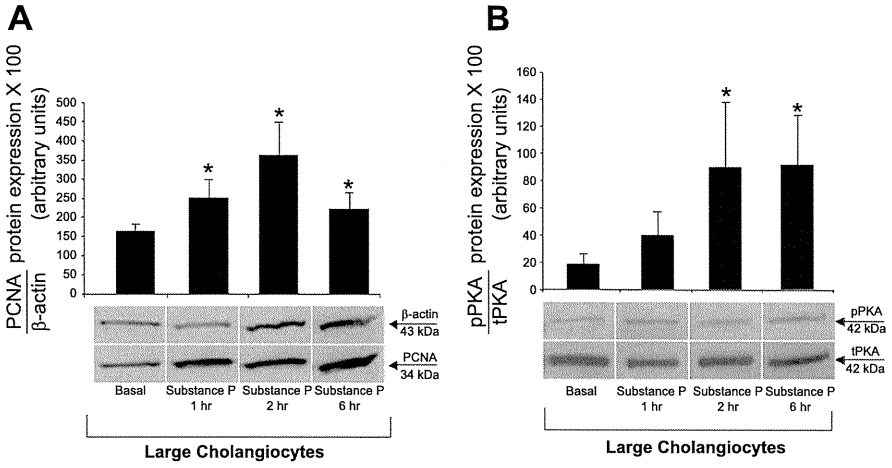


Fig. 8. Effect of 0.2% BSA (basal) or substance P ($10^{-9}$ M for 1, 2, and 6 h) on the proliferation (by PCNA) and phosphorylation of PKA of large cholangiocytes. Substance P increased PCNA protein expression (*A*) and the phosphorylation of PKA (*B*) compared with their corresponding basal values. Data are means ± SE of 10 immunoblots for PCNA (*A*) and 7 immunoblots for PKA derived from protein (10 μg) (*B*) obtained from cumulative preparations of cholangiocytes. *$P < 0.05$ vs. the corresponding value of large cholangiocytes treated with BSA.

stimulate cholangiocyte proliferation during cholestasis. Also, knockout of the secretin receptor gene induces a similar decrease in biliary mass in mice with BDL (22). The reduction of the serum levels of transaminases and bilirubin observed in NK-1R$^{-/-}$ BDL mice further supports the concept that blockage of the NK-1R induced signaling is important in the reduction of liver damage and biliary hyperplasia. The increase in hepatocyte apoptosis and steatosis likely explains the significant increase in the serum levels of transaminases observed in normal NK-1R$^{-/-}$ mice compared with WT normal mice. This finding also suggests that SP signaling may play a role in hepatic metabolism and that lack of the NK-1R may trigger hepatocyte steatosis (41) that was we speculate was resolved during cholestasis induced by BDL. Compared with WT animals, in NK-1R$^{-/-}$ mice a significant reduction in the mRNA expression of collagen 1α and α-SMA after BDL. These data reflect the reduction of the expansion of the biliary tree in NK-1R$^{-/-}$ mice, with a consequent reduction of biliary fibrogenesis, which is mostly likely due to reduced hepatic stellate cell activity (46). In addition to alterations in hepatic stellate cell activation, we cannot rule out that an ancillary part of those differences may be accounted to reduced collagen deposition by hepatocytes, by cholangiocytes, and, in particular, by inflammatory cells, since SP is a one of the mediators of neurogenic inflammation and NK1-R antagonist have been shown to protect mice from cytokine, CD95 and TNF-α mediated liver injury (9, 10).

The biological and pathophysiological significance of our findings is supported by a number of studies. For example, the neurokinin-1 receptor antagonists CP-96,345 and L-733,060 protect mice from cytokine-mediated liver injury, most likely by inhibiting SP effects (10). NK-1R antagonists have been shown to protect mice from CD95- and TNF-α-mediated liver damage (9). As a direct outgrowth of the present study, since a number of neuroendocrine factors regulate biliary functions by autocrine mechanisms, we propose to evaluate the possible autocrine role of SP in the growth and damage of the biliary epithelium.

## ACKNOWLEDGMENTS

We acknowledge Bryan Moss, Scott & White, Medical Illustration Department for assistance with figures, and the Scott & White Hospital animal facility staff assistance with animal surgical models. We thank Anna Webb and the Texas A&M Health Science Center Microscopy Imaging Center for assistance with confocal microscopy.

## GRANTS

This work was supported by the Dr. Nicholas C. Hightower Centennial Chair of Gastroenterology to Dr. Alpini from Scott & White Hospital, a Veterans Affairs (VA) Research Scholar Award, a VA Merit Award, and the National Institute of Diabetes and Digestive and Kidney Diseases (NIDDK) Grant DK062975 to Dr. Alpini. Portions of this study were supported by *1*) by a Scott & White grant award (no. 060483) from Scott & White and the NIDDK RO1 Grant (DK081442) to Dr. Glaser and *2*) a grant from Health and Labor Sciences Research Grants for the Research on Measures for Intractable Diseases (from the Ministry of Health, Labor and Welfare of Japan) and from Grant-in Aid for-Scientific Research C (21590822) from Japan Society for the Promotion of Science to Y. Ueno.

## DISCLOSURES

No conflicts of interest, financial or otherwise, are declared by the author(s).

## REFERENCES

1. **Almeida TA, Rojo J, Nieto PM, Pinto FM, Hernandez M, Martin JD, Candenas ML.** Tachykinins and tachykinin receptors: structure and activity relationships. *Curr Med Chem* 11: 2045–2081, 2004.
2. **Alpini G, Glaser S, Robertson W, Rodgers RE, Phinizy JL, Lasater J, LeSage G.** Large but not small intrahepatic bile ducts are involved in secretin-regulated ductal bile secretion. *Am J Physiol Gastrointest Liver Physiol* 272: G1064–G1074, 1997.
3. **Alpini G, Glaser S, Ueno Y, Pham L, Podila PV, Caligiuri A, LeSage G, LaRusso NF.** Heterogeneity of the proliferative capacity of rat cholangiocytes after bile duct ligation. *Am J Physiol Gastrointest Liver Physiol* 274: G767–G775, 1998.
4. **Alpini G, Lenzi R, Sarkozi L, Tavoloni N.** Biliary physiology in rats with bile ductular cell hyperplasia. Evidence for a secretory function of proliferated bile ductules. *J Clin Invest* 81: 569–578, 1988.
5. **Alpini G, Prall RT, LaRusso NF.** The pathobiology of biliary epithelia. In: *The Liver: Biology & Pathobiology* (4th ed.), edited by Arias IM, Boyer JL, Chisari FV, Fausto N, Jakoby W, Schachter D, and Shafritz DA. Philadelphia, PA: Lippincott Williams & Wilkins, 2001, p. 421–435.
6. **Alpini G, Roberts S, Kuntz SM, Ueno Y, Gubba S, Podila PV, LeSage G, LaRusso NF.** Morphological, molecular, and functional heterogeneity of cholangiocytes from normal rat liver. *Gastroenterology* 110: 1636–1643, 1996.
7. **Alvaro D, Mancino MG, Glaser S, Gaudio E, Marzioni M, Francis H, Alpini G.** Proliferating cholangiocytes: a neuroendocrine compartment in the diseased liver. *Gastroenterology* 132: 415–431, 2007.
8. **Alvaro D, Onori P, Metalli VD, Svegliati-Baroni G, Folli F, Franchitto A, Alpini G, Mancino MG, Attili AF, Gaudio E.** Intracellular pathways

# Enhanced Replication of Hepatitis B Virus With Frameshift in the Precore Region Found in Fulminant Hepatitis Patients

**Jun Inoue, Yoshiyuki Ueno, Yuta Wakui, Koji Fukushima, Yasuteru Kondo, Eiji Kakazu, Masashi Ninomiya, Hirofumi Niitsuma, and Tooru Shimosegawa**

Division of Gastroenterology, Tohoku University Graduate School of Medicine, Sendai, Japan

***Background.*** The genotype B of hepatitis B virus (HBV) was reported to associate with fulminant hepatitis (FH). We aimed to clarify the characteristics of HBV obtained from FH patients in an area of Japan where genotype B HBV is prevalent.

***Methods.*** Using serum samples of 16 HBV-associated FH patients, partial HBV sequences were determined. The effects of HBV mutation/insertion/deletion were evaluated using an in vitro HBV replication system.

***Results.*** Of the 16 HBV isolates, 31% belonged to subgenotype B1/Bj, 38% were subgenotype B2/Ba, and 31% were subgenotype C2/Ce. Notably, the single nucleotide insertion/deletion that resulted in a frameshift of the precore protein was found exclusively in 60% of B1/Bj strains. An in vitro study showed that all of the frameshift mutants had significantly higher amounts of HBV DNA than did the wild type. One of the isolates had a novel insertion of A between nucleotides 1900 and 1901, which resulted in a 3-nucleotide change within the Kozak sequence of the core protein and enhanced the core protein expression in vitro.

***Conclusions.*** The frameshift insertion/deletion in the precore region enhanced HBV replication and might be associated with the development of FH by the subgenotype B1/Bj HBV.

Hepatitis B virus (HBV) is one of the most common viruses affecting the human health. It causes a spectrum of chronic liver diseases including chronic hepatitis, liver cirrhosis, and hepatocellular carcinoma. Acute HBV infection induces acute self-limited hepatitis or fulminant hepatitis (FH), and the pathogenesis leading to the development of fulminant hepatitis B (FHB) is still being investigated. Although enhanced replication of the virus [1, 2] and an exuberant immune response by the host [3] are considered to be the main pathogeneses, various issues are not fully understood.

Received 14 January 2011; accepted 26 May 2011.

Potential conflicts of interest: none reported.

Presented in part: 61th annual meeting of the American Association for the Study of Liver Diseases, Boston, Massachusetts, 29 October–2 November 2010.

Correspondence: Yoshiyuki Ueno, MD, PhD, Division of Gastroenterology, Tohoku University Graduate School of Medicine, 1-1 Seiryo, Aoba-ku, Sendai 980-8574, Japan (yueno@med.tohoku.ac.jp).

**The Journal of Infectious Diseases 2011;204:1017–25**



0022-1899 (print)/1537-6613 (online)/2011/2047-0008$14.00

DOI: 10.1093/infdis/jir485

HBV contains a 3.2-kb, circular, partially double-stranded DNA genome; according to the heterogeneity of the nucleotide sequence, at least 8 (A–H) genotypes [4, 5] and, tentatively, 2 new genotypes (I and J) [6, 7] are classified. HBV genotypes are considered to affect the liver disease outcome [8], and the association of genotype B or subgenotype B1/Bj with FH was reported from Japan [9–11]. It has also been reported that several HBV mutations, such as T1753V (not T), T1754V, A1762T/G1764A, G1862T, G1896A, G1899A, and A2339G, were associated with FH [9–12]. In particular, the mutation of G1896A in the precore region, which makes a stop codon and abrogates hepatitis B e antigen (HBeAg), has been well documented [13–15]. HBV with G1896A was reported to have high replication capacity in vitro [10, 16]. However, in general clinical settings, chronic hepatitis patients with HBV with G1896A, which is the main cause of seroconversion of HBeAg to antibody against HBeAg (HBeAb), have lower viral load [17]. The reason for this discrepancy has not yet been elucidated clearly.

A difference in worldwide geographic distribution of the HBV genotypes has been noted. Also, in Japan, where HBV of genotype C prevails, there is a difference

in the distribution: it is known that the percentage of genotype B is higher in the northeast area [18]. However, little is known about the virological features of HBV obtained from FH patients in this area. Therefore, we aimed to investigate the characteristics of HBV, especially those of genotype B, that cause FH in our hospital in northeast Japan.

## METHODS

### Serum Samples

From January 1996 to November 2010, 60 patients were admitted to our hospital for acute HBV infection. Of them, 15 (25%) were diagnosed with FH. As there was an HBV carrier who developed FH, a total of 16 serum samples from FH patients were used in this study. The diagnosis of FH was made based on the following findings: coma grade II or higher and a prothrombin time <40% developing within 8 weeks after onset.

### Determination of HBV Partial Sequences

The partial sequences of HBV were determined as described previously [19] with modifications. To amplify the 396-nucleotide sequence in the S gene (nucleotides 272–667; the nucleotide numbers are in accordance with a genotype C HBV isolate of 3215 nucleotides [AB033550]), total DNA extracted from 50 μL of serum was subjected to nested polymerase chain reaction (PCR) with the primers described previously. To amplify the 255-nucleotide sequence in the core promoter/precore region (nucleotides 1673–1927), the first round of PCR was carried out with primers B015 (5'-CAC GTY GCA TGG ARA CCA CCG TGA-3' [Y = C or T; R = A or G]) and B008 (5'-GTC AGA AGG CAA AAA AGA GAG TAA CTC-3'), and the second round was carried out with primers B016 (5'-GTC TTR CAT AAG AGG ACT CTT GGA CT-3') and B007 (5'-AAA GAG AGT AAC TCC ACA GAA GCT CC-3'). The amplification products were sequenced on both strands directly on an ABI PRISM 3100 Genetic Analyzer (Applied Biosystems), located in the Biomedical Research Core of Tohoku University Graduate School of Medicine. Sequence analysis and evaluation of the epsilon (ϵ) signal stability, which was calculated as minimum free energy, were performed using Genetyx-Mac (Version 12.2.6; Genetyx Corp). The sequence data from the current report have been assigned to the GenBank/EMBL/DDBJ with the accession numbers AB602749–AB602759 (partial S region sequence) and AB602760–AB602770 (partial core promoter/precore sequence).

### Construction of Plasmids

A plasmid containing the 1.3-fold HBV genome (nucleotide 1051-3215/1-1953) was constructed as described previously [20] using serum of a self-limited acute hepatitis patient (AH-2; accession number of the full-genome sequence, AB602818) with HBV of the subgenotype B1/Bj in our hospital. Because the isolate had a mutation of G1899A in the precore region, the mutation was converted to the wild-type nucleotide using Quick Change II-E Site-Directed Mutagenesis Kit (Stratagene) as described previously [20], and the clone was used as a subgenotype B1/Bj wild-type clone.

The wild clone was used as template to construct a clone with a mutation of G1896A, an insertion of A between nucleotides 1837 and 1838 (1838insA), a deletion of a single nucleotide at 1846 (1846del), or an insertion of A between nucleotides 1900 and 1901 (1901insA). A clone with 1901insA was used as the next template to introduce the additional mutation of T1855C. All constructs were sequenced to confirm the introduced mutation/insertion/deletion.

### Cell Culture and Transfection

Human hepatoma HepG2 cells were cultured as described previously [20]. On the next day, after seeding cells in 24-well plates at $1.25 \times 10^5$ cells/well, 0.5 μg/well of plasmid DNA was transfected using FuGENE HD Transfection Reagent (Roche Diagnostics), and the culture supernatant and cells were collected 3 days later. For Southern blot analysis, cells were seeded in 6-well plates at $5.0 \times 10^5$ cells/well, and 1.5 μg/well of plasmid DNA was transfected. In this system, the transfection efficiency could be evaluated with the level of hepatitis B surface antigen (HBsAg) in the culture supernatant [20]. The experiments were performed at least in triplicate.

### Assay of HBV Markers

Five microliters of the supernatant was treated with 5 units of DNase I (TaKaRa Bio) at 37°C for 2 hours to digest the input plasmid DNA in the culture supernatant, and the reaction was stopped with ethylenediaminetetraacetic acid. Then, total DNA was extracted with a QIAamp DNA Blood Mini Kit (QIAGEN GmbH), and the amount of HBV DNA was quantified with real-time PCR using a StepOnePlus Real Time PCR System (Applied Biosystems) [21]. HBsAg and HBeAg in 50 μL of the culture supernatant were assayed by enzyme-linked immunosorbent assay [20]. To detect the intracellular replicative intermediates of HBV, the core particle–associated HBV DNA in the cells was isolated as described previously [20]. After DNase I treatment for the removal of unprotected DNA, extracted total DNA was analyzed by Southern blotting using a full-length HBV DNA probe labeled with PCR DIG Probe Synthesis Kit (Roche Diagnostics).

### In Vitro Cell-Free Protein Expression

To investigate whether the change of the Kozak sequence around the initiation codon of the core protein affects the protein expression, TNT T7 Quick for PCR DNA (Promega) was used. The template of transcription/translation was a purified PCR product that was amplified from the subgenotype B1/Bj wild clone. To make the wild-type template, PCR was performed with a forward primer CoreKW (5'-GGA TCC TAA TAC GAC TCA CTA TAG

GGA ACA TGG GGC ATG GAC ATT GAC CCT T-3'), including the T7 promoter sequence, spacer, and the Kozak sequence (underlined) including the initiation codon of the core protein, followed by the partial core sequence and a reverse primer CoreR (5'-CTA TCT AGA CTA ACA TTG GGA TTC CCG A-3') including the termination codon of the core protein. To make templates with G1896A, G1899A, and 1901insA, forward primers CoreK-5A (the underlined sequence of CoreKW was changed to TAGGGCATGG), CoreK-2A (the underlined sequence was changed to TGGGACATGG), and CoreK-1A-2C-6G (the underlined sequence was changed to GGGGCAATGG) were used, respectively. The expressed protein was analyzed with Western blotting using a rabbit polyclonal anti–hepatitis B core antigen (HBcAg) antibody (Dako) as the primary antibody.

### Statistical Analysis

Statistical analyses were performed using Mann–Whitney $U$ test for comparison of continuous variables between 2 groups. Differences were considered to be statistically significant when $P < .05$.

## RESULTS

### Characteristics of the Fulminant Hepatitis Patients

The clinical characteristics of the 16 FH patients are shown in Table 1. The mean age was 53.0 years (range, 29–71), and 13 (81%) were male. The mean peak total bilirubin was 14.7, the mean peak alanine aminotransferase was 4932, and the mean lowest prothrombin time was 18.6%. Nine (56%) patients died of fulminant hepatitis. Lamivudine was administered to 4 patients (numbers 12–15), and entecavir was administered to 1 patient (number 16). After 2003, living related liver transplantation has been performed for 4 FH patients, and all of the patients were rescued. Two of them (numbers 12 and 13) showed rapid progression and were considered so-called hyperacute cases, but were rescued with liver transplantation without complications [22]. The HBV isolates from these patients were named BFJT followed by the onset year, excluding 5 cases referred to as FH-1 to FH-5 in a previous report by us [23].

### Determination of HBV Genotype

Based on the partial sequences in the S region of HBV isolates from FH patients, a phylogenetic tree was constructed (Figure 1). Of the 16 HBV isolates, 5 (31%) belonged to subgenotype B1/Bj, 6 (38%) belonged to subgenotype B2/Ba, and 5 (31%) were subgenotype C2/Ce. The 5 isolates of subgenotype B2/Ba were grouped into a cluster: these patients were considered to have the same source of infection [23]. In this study, 69% of the FH patients were infected with genotype B HBV, which was much higher than previously reported in Japan (22%–33%) [10, 11]. It was also higher than the reported percentage (21%) of genotype B in acute hepatitis B patients in northeast Japan [24].

### Mutation, Insertion, and Deletion in the Core Promoter and Precore Region

The analysis of the partial sequences in the core promoter/precore region showed that there were several mutations in the HBV isolates. The mutations that were reported previously to have an association with FH are shown in Table 2. Because the 5 isolates of subgenotype B2/Ba were almost identical, they were counted as a single strain. The mutations at nucleotides 1753,

**Table 1. Characteristics of the Fulminant Hepatitis B Patients**

| Patient no. | Age/sex | Date of onset | Peak T. Bil (mg/dL) | Peak ALT (IU/L) | Lowest PT (%) | Possible infection source | Liver transplantation | Outcome | HBV isolate name |
|---|---|---|---|---|---|---|---|---|---|
| 1 | 65/M | December 1996 | 19.2 | 1764 | 18.0 | Unknown | No | Died | BFJT1996-1 |
| 2 | 29/M | October 1997 | 8.8 | 6900 | 5.0 | Unknown | No | Died | BFJT1997-1 |
| 3 | 65/M | February 1999 | 16.9 | 2162 | 22.4 | Unknown | No | Died | BFJT1999-1 |
| 4 | 28/F | August 1999 | 8.9 | 7120 | 17.1 | Sexual contact | No | Rescued | BFJT1999-2 |
| 5 | 61/M | May 2000 | 32.8 | 3750 | 26.0 | Unknown | No | Died | BFJT2000-1 |
| 6 | 69/F | May 2000 | 10.6 | 4190 | 6.0 | Iatrogenic | No | Died | FH-1 |
| 7 | 71/M | July 2000 | 29.0 | 3530 | 38.0 | Iatrogenic | No | Died | FH-2 |
| 8 | 66/M | October 2000 | 13.9 | 6950 | 10.1 | Iatrogenic | No | Died | FH-3 |
| 9 | 50/M | December 2000 | 13.3 | 13 420 | 10.0 | Blood transfusion | No | Died | BFJT2000-2 |
| 10 | 71/F | December 2000 | 17.0 | 3380 | 27.0 | Iatrogenic | No | Rescued | FH-4 |
| 11 | 60/M | February 2001 | 6.4 | 10 290 | 12.7 | Iatrogenic | No | Died | FH-5 |
| 12 | 45/M | July 2003 | 11.8 | 6450 | 9.3 | Sexual contact | Yes | Rescued | BFJT2003-1 |
| 13 | 34/M | August 2003 | 9.5 | 7150 | 9.0 | Sexual contact | Yes | Rescued | BFJT2003-2 |
| 14 | 32/M | July 2005 | 10.8 | 278 | 22.1 | Sexual contact | Yes | Rescued | BFJT2005-1 |
| 15 | 38/M | August 2006 | 5.1 | 728 | 39.8 | Unknown | No | Rescued | BFJT2006-1 |
| 16 | 64/M | April 2009 | 20.5 | 857 | 24.7 | Carrier | Yes | Rescued | BFJT2009-1 |

**NOTE.** ALT, alanime aminotransferase; HBV, hepatitis B virus; PT, prothrombin time; T. Bil, tital bilirubin.

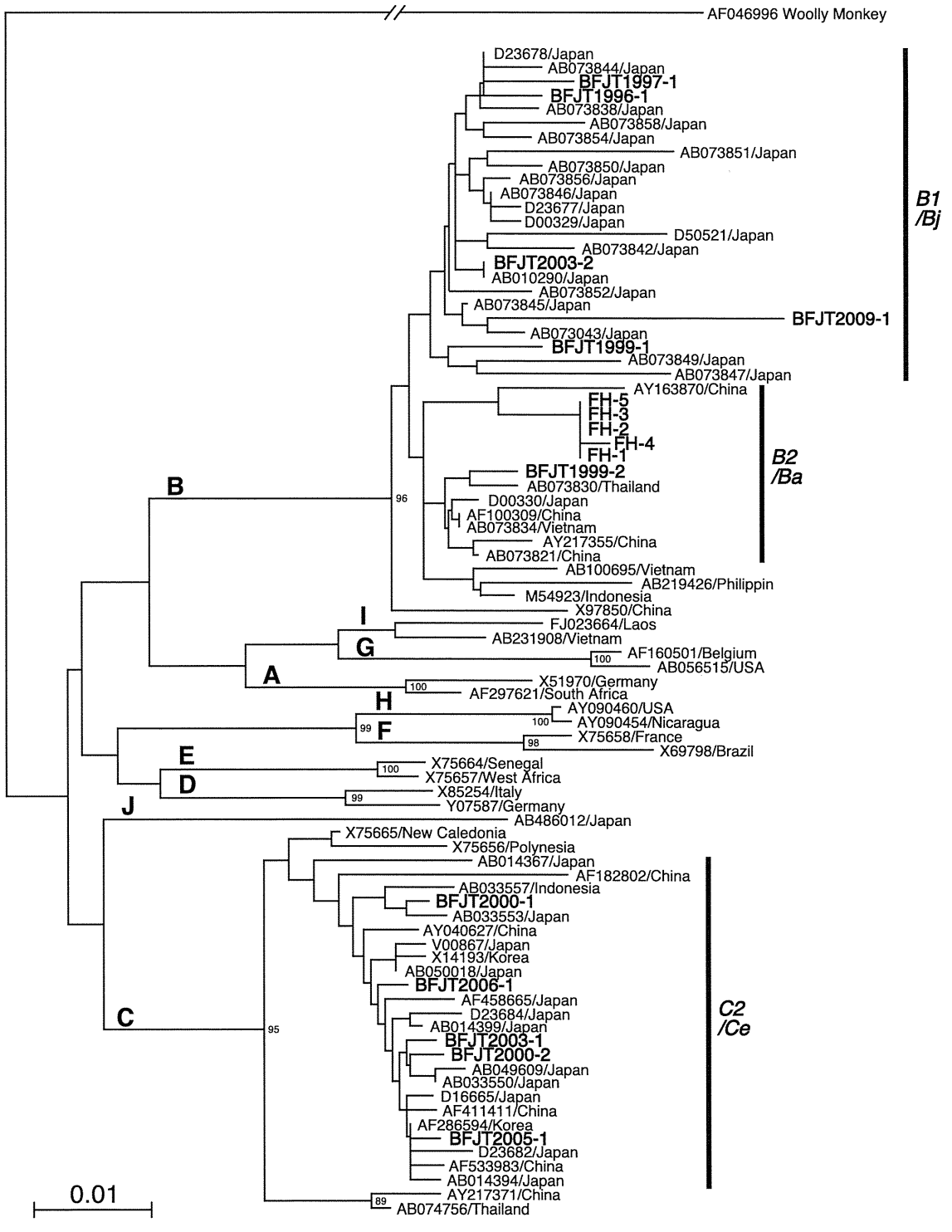


**Figure 1.** Phylogenetic tree constructed by the neighbor-joining method based on the partial 396-nucleotide sequences in the S region of 84 hepatitis B virus isolates. In addition to the 16 isolates found in this study, which are indicated in bold type for visual clarity, 68 reported isolates of genotypes A–J were included for comparison. Bootstrap values are indicated for the major nodes as a percentage obtained from 1000 resamplings of the data.

1754, 1762/1764, 1862, 1896, and 1899 were found in 17%, 33%, 42%, 8%, 67%, and 25% of the 12 isolates, respectively. Among the subgenotypes, there were differences in the distribution of the mutations: T1754G was found only in subgenotype B1/Bj (4 of 5, 80%), the mutations at nucleotide 1762/1764 were found in subgenotype B2/Ba and C2/Ce (5 of 7, 71%), and G1899A was found only in subgenotype B1/Bj (3 of 5, 60%). Interestingly, an insertion/deletion of a single nucleotide in the precore region (1838insA, 1846del, and 1901insA) was also found only in subgenotype B1/Bj (3 of 5, 60%). The surrounding nucleotide

**Table 2. Mutations, Insertions, and Deletions of Hepatitis B Virus Found in the Fulminant Hepatitis Patients**

| Isolate name | Subgenotype | Nucleotide no.[a] | | | | | | Frameshift[b] |
|---|---|---|---|---|---|---|---|---|
| | | 1753 | 1754 | 1762/1764 | 1862 | 1896 | 1899 | |
| BFJT1996-1 | B1/Bj | T | T | A/G | G | G | **A** | **1846del** |
| BFJT1997-1 | B1/Bj | T | **G** | A/G | G | G | G | **1901insA** |
| BFJT1999-1 | B1/Bj | T | **G** | A/G | G | **A** | **A** | ... |
| BFJT2003-2 | B1/Bj | T | **G** | A/G | G | **A** | G | **1838insA** |
| BFJT2009-1 | B1/Bj | **Y** | **G** | A/G | G | **A** | **A** | ... |
| BFJT1999-2 | B2/Ba | T | T | A/G | G | **A** | G | ... |
| FH-1,2,3,4,5[c] | B2/Ba | T | T | **T/A** | **T** | **A** | G | ... |
| BFJT2000-1 | C2/Ce | T | T | **T/A** | G | **A** | G | ... |
| BFJT2000-2 | C2/Ce | T | T | **T/A** | G | **A** | G | ... |
| BFJT2003-1 | C2/Ce | T | T | A/**A** | G | **A** | G | ... |
| BFJT2005-1 | C2/Ce | **G** | T | **T/A** | G | G | G | ... |
| BFJT2006-1 | C2/Ce | T | T | A/G | G | G | G | ... |
| Frequency (%) | | 17 | 33 | 42 | 8 | 67 | 25 | 25 |

**NOTE.** 1846del, a single nucleotide deletion at nucleotide 1846; 1901insA, an insertion of A between nucleotide 1900 and 1901; 1838insA, an insertion of A between nucleotide 1837 and 1838.

[a] The nucleotides of mutation are indicated in bold type.

[b] Insertion/deletion that causes a frameshift in the precore protein.

[c] These isolates are indicated as a single strain because of the high identity [23].

sequences of the single nucleotide insertions/deletions in this study are shown in Figure 2. The insertions in this region make a termination codon at nucleotide 1909 or 1915 in a frame of the precore protein, and the deletion makes a termination codon at nucleotide 1993. Therefore, these single nucleotide insertions/deletions resulted in frameshifts of the precore protein, and they were thought to abrogate HBeAg expression. These precore frameshift mutants were previously found in HBeAg-negative HBV carriers [25, 26]. As for self-limited acute hepatitis B patients, we found that only 1 of 96 (1%) patients had the frameshift mutant (data not shown).

With the aim of clarifying the distribution of the precore frameshift insertion/deletion in the general population, the HBV isolates whose entire sequences were known were retrieved from the Hepatitis Virus Database [27]. In November 2010, a total of 3457 full-length sequences of HBV were registered, and of these, 3391 sequences were proved to belong to genotypes A–I based on a phylogenetic tree analysis. In total, 11 (0.3%) isolates with the precore frameshift were found in genotypes A, B, C, and D isolates (Table 3). Therefore, the frameshift seemed to be rare in general, but can occur in several genotypes other than genotype B.

Of the mutations, insertions, and deletion in the precore region found in the FH patients, G1896A, G1899A, and 1901insA can affect the ϵ signal of HBV. The ϵ signal, which forms a secondary structure of pregenomic RNA, is highly conserved among HBV strains and is essential for the initiation of the encapsidation of pregenomic RNA [28]. Figure 2 depicts the structure of the ϵ signal with G1896A and G1899A, which stabilize the nucleotide pair in the lower stem. The stabilized ϵ signal has an advantage for pregenomic RNA encapsidation [28] and is considered to lead to heightened replication efficiency of HBV. However, 1901insA distorted the secondary structure of the lower stem and seemed to make the ϵ signal wobble (Figure 2). The mutation of T1855C, which might compensate for the instability, was present along with 1901insA in the BFJT1997-1 isolate. The change of the ϵ signal stability was evaluated by calculating the minimum free energy (Figure 2): the lower energy value indicates higher stability of the structure. It was indicated that the ϵ signal with G1896A and/or G1899A had higher stability than the wild type. The structure with 1901insA has lower stability, and it was confirmed that the mutation of T1855C restores the stability, which was still lower than that of the wild type.

### Effect of the Precore Frameshift on HBV Replication In Vitro

To confirm whether the frameshift in the precore region of subgenotype B1/Bj HBV has significance in the development of FH, the replication capacity of the HBV clones with the frameshift insertion/deletion (1838insA, 1846del, and 1901insA) was evaluated in vitro using plasmids containing the 1.3-fold HBV genome (Figure 3). As expected, the level of HBsAg in the culture supernatant was almost equal, and the HBeAg level of the clones with the frameshift was significantly lowered to the same level as the clones with G1896A, which is known to abrogate HBeAg. When the amount of HBV DNA in the culture supernatant was assayed, it was revealed that the clones with the frameshift had significantly higher HBV DNA levels than did the wild type. The HBV DNA level of the clone with G1896A ± G1899A was significantly higher, also.

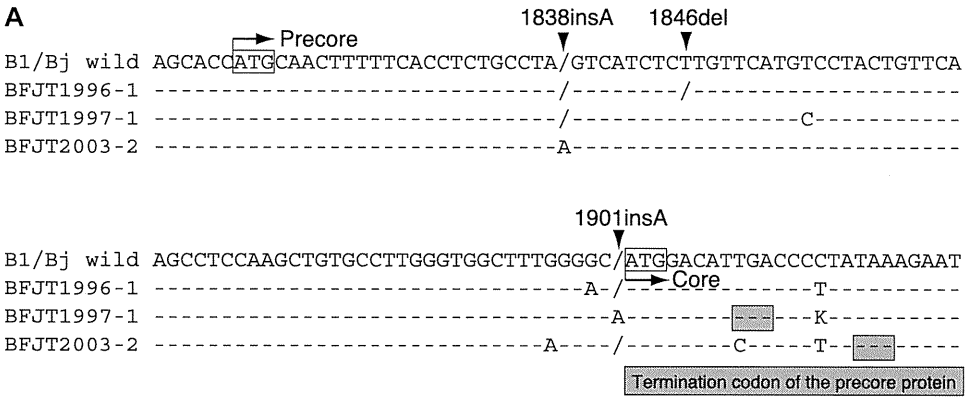


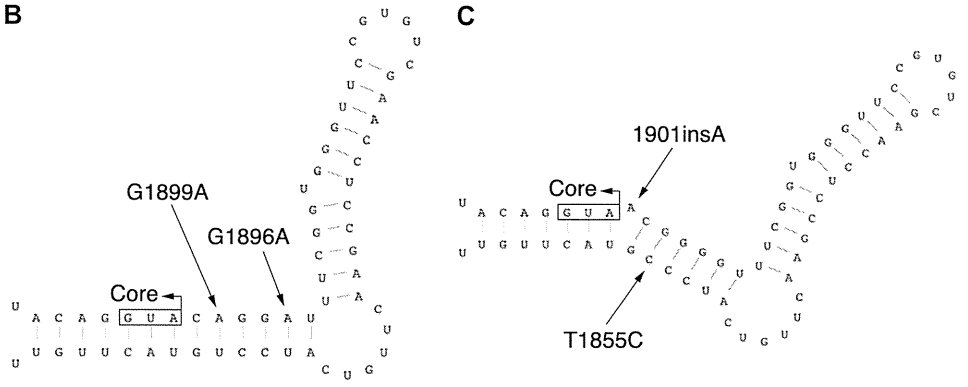


D

| Mutation/insertion in the ε signal | Minimum free energy (kcal/mol) |
|---|---|
| B1/Bj wild type (D00329) | -24.9 |
| G1896A | -25.5 |
| G1899A | -26.1 |
| G1896A+G1899A | -26.7 |
| 1901insA | -21.0 |
| 1901insA+T1855C | -24.1 |

**Figure 2.** *A*, Partial sequences around the precore region of hepatitis B virus (HBV) with frameshift insertion/deletion obtained in this study. The sequence (nucleotides 1808–1925) of a subgenotype B1/Bj wild-type isolate (D00329) is shown on the first line for comparison. The white boxes indicate the initiation codons of the precore/core protein, and the gray boxes indicate the termination codons of the precore protein resulting from the frameshift insertions. *B*, Secondary structure of the ϵ signal of HBV pregenomic RNA with the mutations of both G1896A and G1899A, which are found commonly in fulminant hepatitis patients and hepatitis B e antigen (HBeAg)–negative carriers. *C*, Secondary structure of the ϵ signal with both 1901insA and T1855C found in the BFJT1997-1 isolate. *D*, Stability of the ϵ signal evaluated with minimum free energy, which was calculated using Genetyx Mac. The mutation/insertion was assumed to be present in the B1/Bj wild-type sequence (D00329) and analyzed.

Because the BFJT1997-1 isolate with 1901insA had T1855C in the precore region, the effect of the mutation on HBV replication was evaluated (Figure 3). Interestingly, T1855C increased significantly the HBV DNA level of the clone with 1901insA. The clone with T1855C without 1901insA did not increase the HBV DNA level in comparison with that of the wild type. Therefore, the effect of T1855C was considered to be a restoration of the ϵ signal instability with 1901insA as described above.

The amount of the intracellular replicative intermediates of HBV was evaluated with Southern blot analysis (Figure 3). The result was concordant with that of the HBV DNA level in the culture supernatant. This indicated that the precore frameshift had an effect in the replication cycle before the release step of virion, such as the encapsidation of pregenomic RNA.

### Change of the Core Protein Expression Level With the Frameshift Insertion

Although it is considered that the stability of the ϵ signal is necessary for efficient replication [28], the structure of the ϵ signal with 1901insA and T1855C seemed not to be more stable than the wild type as shown in Figure 2. Therefore, another mechanism by which the HBV replication is enhanced was assumed

**Table 3. Distribution of Insertions and Deletions That Cause Frameshift of the Precore Protein Among HBV Genotypes A–I, Based on the Isolates Whose Full-length Sequences Were Known**

| | | | Subgenotype | | | | | | | | | |
|---|---|---|---|---|---|---|---|---|---|---|---|---|
| Genotype[a] | A | B | B1 | B2 | C | D | E | F | G | H | I | Total |
| No. | 427 | 856 | 40 | 659 | 1191 | 499 | 249 | 77 | 26 | 30 | 36 | 3391 |
| Insertion | 2 | 1 | 1 | 0 | 1 | 1 | 0 | 0 | 0 | 0 | 0 | 5 |
| Deletion[b] | 1 | 2 | 0 | 2 | 3 | 0 | 0 | 0 | 0 | 0 | 0 | 6 |
| Total (%) | 3 | 3 | 1 | 2 | 4 | 1 | 0 | 0 | 0 | 0 | 0 | 11 |
| | (0.7) | (0.4) | (2.5) | (0.3) | (0.3) | (0.2) | (0) | (0) | (0) | (0) | (0) | (0.3) |

**NOTE.** HBV, hepatitis B virus.

[a] If the recombination of the genome among different genotypes was present, the genotype of HBV was determined by the phylogenetic tree analysis based on the full-length HBV sequences.

[b] The isolates that had deletions including the precore initiation codon were not counted as having the frameshift deletion.

to act. We focused on the change of the Kozak sequence around the initiation codon of the core protein. The Kozak sequence includes the 6-nucleotide sequence just before the initiation codon and 1-nucleotide after that (optimal sequence, GCCA/GCCATGC), and it affects the translation efficiency [29]. Figure 4 shows the altered Kozak sequence of the core protein with G1896A, G1899A, and 1901insA. Whereas G1896A and G1899A make a 1-nucleotide change in the Kozak sequence, 1901insA makes a 3-nucleotide change. A cell-free protein expression system was used to clarify whether the Kozak sequence alteration affects the core protein expression. Western blot analysis of the expressed core protein showed that the Kozak sequence with G1896A or G1899A increased the expression slightly in comparison with the wild-type sequence and, notably, that the Kozak sequence with 1901insA increased the protein level greatly (Figure 4). This increment of the core protein may enhance the replication of HBV particles and may lead to the development of FH.

## DISCUSSION

It has been considered that FHB results from the rapid increase of HBV and the vigorous host immune response to HBV-infected hepatocytes [30, 31]. Several mutations found in HBV of FH patients were reported to enhance the HBV replication in vitro [1, 10]. We previously reported that a FH strain caused intracellular retention of HBV, which was thought to be associated with pathogenesis [20]. Here, we described that the single nucleotide insertion/deletion in the precore region leading to a frameshift, which abrogates HBeAg, was found frequently in our FH patients with subgenotype B1/Bj HBV. The frameshift mutants had never been reported in self-limited acute hepatitis patients, whose HBeAg-positive rate is high (56%–84%) [10, 11, 32, 33]. The number of patients in this study was small, but the significance of the frameshift could be confirmed using an in vitro HBV replication system. Although HBV isolates with the frameshift were rarely found in general, patients with acute infection with these isolates may be at risk of developing FH.

This study showed that genotype B HBV was found frequently (69%) in the FHB patients in our hospital in northeast Japan. Recently, the frequency of genotype B in chronic hepatitis B patients in northeast Japan was reported to be higher than that in all Japan (44% vs 14%, respectively) [18]. Although the percentage of genotype B in FHB patients in the area had not reported, this study confirmed that the genotype B percentage was higher. Whereas genotype B HBV frequently leads to FH [9–11], it causes less progressive chronic liver disease than genotype C. This phenomenon was considered to link to earlier HBeAg/Ab seroconversion in the natural course of genotype B compared with that of genotype C [34].

In this study, the precore frameshift was found exclusively in subgenotype B1/Bj strains. The database search showed that the frameshift could occur in several genotypes, at least genotypes A–D, but not frequently (0.3% in total). Interestingly, a previous report by Sugauchi et al showed that 7 of 275 (2.5%) chronically infected patients with subgenotype B1/Bj had the frameshift insertion of 1838insA [35]. Because the number of genotype B1/Bj isolates in that report is larger than that from the database search of full-length HBV sequences, this frequency is more convincing. This may be one of the reasons why subgenotype B1/Bj HBV frequently causes FH.

Previous reports described that HBV with G1896A had a high replication capacity [10], and the present study showed that the precore frameshift insertion/deletion also enhanced the HBV replication to the same level as G1896A. It was reported that p22, the N-terminal-processed p25 precore protein, inhibited the formation of nucleocapsids and regulated the HBV replication [16]. The protein of p22 is further modified at the C-terminal region to secrete p17 HBeAg. HBV with G1896A or the frameshift insertion/deletion in the precore region does not express p25 and the resulting p22. If there is no p22, the nucleocapsids are formed efficiently and the replication of HBV particles can be accelerated. However, this contravenes the general course of HBV carriers, whose seroconversion of HBeAg/HBeAb leads to the reduction of serum HBV DNA

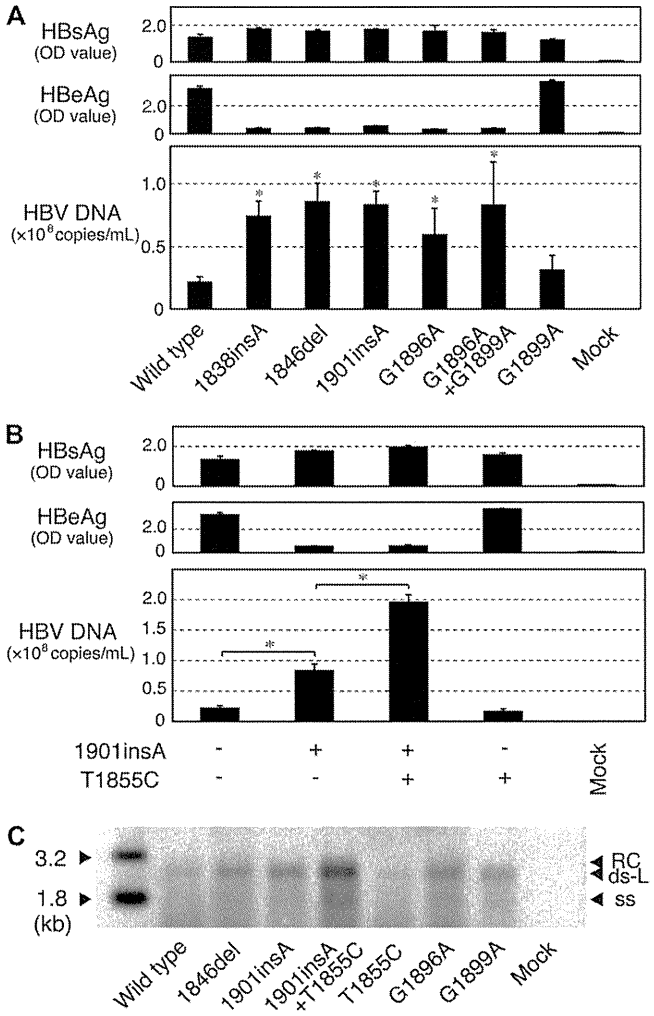


**Figure 3.** *A*, Level of hepatitis B surface antigen (HBsAg), hepatitis B e antigen (HBeAg), and hepatitis B virus (HBV) DNA in the culture supernatant of HepG2 cells that were transfected with several HBV constructs with a frameshift insertion/deletion or mutations in the precore region. *, $P < .05$ in comparison with the wild type. *B*, Level of HBsAg, HBeAg, and HBV DNA in the culture supernatant of HepG2 cells transfected with HBV constructs with 1901insA and/or T1855C. *, $P < .05$. *C*, Representative data of the intracellular replicative intermediates of HBV detected with Southern blot analysis. ds-L, double-stranded linear HBV DNA; OD, optical density; RC, relaxed-circular HBV DNA; ss, single-stranded HBV DNA.

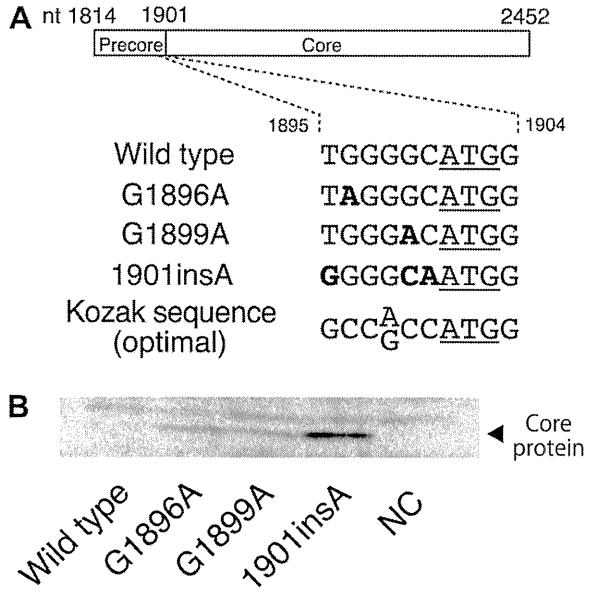


**Figure 4.** *A*, Schema of the Kozak sequence around the initiation codon of the core protein. The changed nucleotides in the Kozak sequene, which were found in hepatitis B virus (HBV) with G1896A, G1899A, or 1901insA, are shown in bold type. *B*, Results of Western blot analysis of the expressed HBV core protein in a cell-free protein expression system. NC, negative control.

[17]. The discrepancy may be due to the adaptive immune response in HBV carriers. Under the suppression by cytotoxic T lymphocytes, HBeAg-negative HBV clones, which have an advantage in the replication cycle, may be barely persistent in the late phase of HBV infection.

The ϵ signal of HBV pregenomic RNA is recognized by HBV polymerase, and both of them are encapsidated into the core particle [36]. Stability of the ϵ signal favors replication [28] and, therefore, G1896A and G1899A may easily occur in the natural course of HBV infection. However, 1901insA, which was found in an FH patient, degrades the stability. It was compensated by a distinct mutation of T1855C, but seemed not to be so stable based on the secondary structure of the ϵ signal. This in vitro study revealed that the enhancement of HBV replication by the novel insertion of 1901insA resulted from the change of the Kozak sequence of the core protein. It was also interesting that G1896A and G1899A increased the core protein expression level slightly. As for the Kozak sequence in HBV, the sequence just upstream of the precore initiation codon was described previously [37]: it affects the expression of HBeAg, and associates with the seroconversion of HBeAg/Ab. There is a possibility that the Kozak sequence of other HBV proteins such as polymerase, HBsAg, and X protein may alter the HBV replication capacity or the disease outcome.

In conclusion, the frameshift insertion/deletion in the precore region was found frequently in subgenotype B1/Bj HBV from FH patients in northeast Japan. The frameshift was shown to enhance the HBV replication in vitro and, in particular, the insertion of 1901insA heightened the replication capacity via the novel mechanism of the changed Kozak sequence of the core protein. Therefore, the precore frameshift may have significance in the development of FH.

## Funding

This work was supported in part by a Grant-in-Aid for Young Scientists (B) (22790627) from the Ministry of Education, Culture, Sports, Science, and Technology of Japan, and grants from the Ministry of Health, Labor, and Welfare of Japan.

## References


1. Hasegawa K, Huang J, Rogers SA, Blum HE. Liang TJ. Enhanced replication of a hepatitis B virus mutant associated with an epidemic of fulminant hepatitis. J Virol **1994**; 68:1651–9.
2. Baumert TF, Rogers SA, Hasegawa K, Liang TJ. Two core promotor mutations identified in a hepatitis B virus strain associated with fulminant hepatitis result in enhanced viral replication. J Clin Invest **1996**; 98:2268–76.
3. Rivero M, Crespo J, Fabrega E, et al. Apoptosis mediated by the Fas system in the fulminant hepatitis by hepatitis B virus. J Viral Hepat **2002**; 9:107–13.
4. Okamoto H, Tsuda F, Sakugawa H, et al. Typing hepatitis B virus by homology in nucleotide sequence: comparison of surface antigen subtypes. J Gen Virol **1988**; 69:2575–83.
5. Norder H, Courouce AM, Coursaget P, et al. Genetic diversity of hepatitis B virus strains derived worldwide: genotypes, subgenotypes, and HBsAg subtypes. Intervirology **2004**; 47:289–309.
6. Olinger CM, Jutavijittum P, Hubschen JM, et al. Possible new hepatitis B virus genotype, southeast Asia. Emerging Infect Dis **2008**; 14: 1777–80.
7. Tatematsu K, Tanaka Y, Kurbanov F, et al. A genetic variant of hepatitis B virus divergent from known human and ape genotypes isolated from a Japanese patient and provisionally assigned to new genotype. J Virol **2009**; 83:10538–47.
8. Kao JH, Chen PJ, Lai MY, Chen DS. Hepatitis B genotypes correlate with clinical outcomes in patients with chronic hepatitis B. Gastroenterology **2000**; 118:554–9.
9. Imamura T, Yokosuka O, Kurihara T, et al. Distribution of hepatitis B viral genotypes and mutations in the core promoter and precore regions in acute forms of liver disease in patients from Chiba, Japan. Gut **2003**; 52:1630–7.
10. Ozasa A, Tanaka Y, Orito E, et al. Influence of genotypes and precore mutations on fulminant or chronic outcome of acute hepatitis B virus infection. Hepatology **2006**; 44:326–34.
11. Kusakabe A, Tanaka Y, Mochida S, et al. Case-control study for the identification of virological factors associated with fulminant hepatitis B. Hepatol Res **2009**; 39:648–56.
12. Hou J, Lin Y, Waters J, et al. Detection and significance of a G1862T variant of hepatitis B virus in Chinese patients with fulminant hepatitis. J Gen Virol **2002**; 83:2291–8.
13. Kosaka Y, Takase K, Kojima M, et al. Fulminant hepatitis B: induction by hepatitis B virus mutants defective in the precore region and incapable of encoding e antigen. Gastroenterology **1991**; 100:1087–94.
14. Liang TJ, Hasegawa K, Rimon N, Wands JR, Ben-Porath E. A hepatitis B virus mutant associated with an epidemic of fulminant hepatitis. N Engl J Med **1991**; 324:1705–9.
15. Omata M, Ehata T, Yokosuka O, Hosoda K, Ohto M. Mutations in the precore region of hepatitis B virus DNA in patients with fulminant and severe hepatitis. N Engl J Med **1991**; 324:1699–704.
16. Scaglioni PP, Melegari M, Wands JR. Posttranscriptional regulation of hepatitis B virus replication by the precore protein. J Virol **1997**; 71: 345–53.
17. Fattovich G, Bortolotti F, Donato F. Natural history of chronic hepatitis B: special emphasis on disease progression and prognostic factors. J Hepatol **2008**; 48:335–52.
18. Matsuura K, Tanaka Y, Hige S, et al. Distribution of hepatitis B virus genotypes among patients with chronic infection in Japan shifting toward an increase of genotype A. J Clin Microbiol **2009**; 47:1476–83.
19. Takahashi M, Nishizawa T, Gotanda Y, et al. High prevalence of antibodies to hepatitis A and E viruses and viremia of hepatitis B, C, and D viruses among apparently healthy populations in Mongolia. Clin Diagn Lab Immunol **2004**; 11:392–8.
20. Inoue J, Ueno Y, Nagasaki F, et al. Enhanced intracellular retention of a hepatitis B virus strain associated with fulminant hepatitis. Virology **2009**; 395:202–9.
21. Liu Y, Hussain M, Wong S, Fung SK, Yim HJ, Lok AS. A genotype-independent real-time PCR assay for quantification of hepatitis B virus DNA. J Clin Microbiol **2007**; 45:553–8.
22. Inoue J, Ueno Y, Kanno N, et al. Living related liver transplantation for acute fulminant hepatitis B: experience from two possible hyper-acute cases. Tohoku J Exp Med **2005**; 205:197–204.
23. Nagasaki F, Ueno Y, Niitsuma H, et al. Analysis of the entire nucleotide sequence of hepatitis B causing consecutive cases of fatal fulminant hepatitis in Miyagi prefecture Japan. J Med Virol **2008**; 80: 967–73.
24. Sugauchi F, Orito E, Ohno T, et al. Spatial and chronological differences in hepatitis B virus genotypes from patients with acute hepatitis B in Japan. Hepatol Res **2006**; 36:107–14.
25. Santantonio T, Jung MC, Miska S, Pastore G, Pape GR, Will H. High prevalence and heterogeneity of HBV preC mutants in anti-HBe-positive carriers with chronic liver disease in southern Italy. J Hepatol **1991**; 13(Suppl 4):S78–81.
26. Okamoto H, Yotsumoto S, Akahane Y, et al. Hepatitis B viruses with precore region defects prevail in persistently infected hosts along with seroconversion to the antibody against e antigen. J Virol **1990**; 64: 1298–303.
27. Shin IT, Tanaka Y, Tateno Y, Mizokami M. Development and public release of a comprehensive hepatitis virus database. Hepatol Res **2008**; 38:234–43.
28. Lok AS, Akarca U, Greene S. Mutations in the pre-core region of hepatitis B virus serve to enhance the stability of the secondary structure of the pre-genome encapsidation signal. Proc Natl Acad Sci U S A **1994**; 91:4077–81.
29. Kozak M. At least six nucleotides preceding the AUG initiator codon enhance translation in mammalian cells. J Mol Biol **1987**; 196:947–50.
30. Inoue J. Factors involved in the development of fulminant hepatitis B: are the mutations of hepatitis B virus implicated? Hepatol Res **2009**; 39:1053–5.
31. Milich D, Liang TJ. Exploring the biological basis of hepatitis B e antigen in hepatitis B virus infection. Hepatology **2003**; 38: 1075–86.
32. Sainokami S, Abe K, Sato A, et al. Initial load of hepatitis B virus (HBV), its changing profile, and precore/core promoter mutations correlate with the severity and outcome of acute HBV infection. J Gastroenterol **2007**; 42:241–9.
33. Ogawa M, Hasegawa K, Naritomi T, Torii N, Hayashi N. Clinical features and viral sequences of various genotypes of hepatitis B virus compared among patients with acute hepatitis B. Hepatol Res **2002**; 23:167–77.
34. Chu CJ, Hussain M, Lok AS. Hepatitis B virus genotype B is associated with earlier HBeAg seroconversion compared with hepatitis B virus genotype C. Gastroenterology **2002**; 122:1756–62.
35. Sugauchi F, Kumada H, Sakugawa H, et al. Two subtypes of genotype B (Ba and Bj) of hepatitis B virus in Japan. Clin Infect Dis **2004**; 38: 1222–8.
36. Ryu DK, Kim S, Ryu WS. Hepatitis B virus polymerase suppresses translation of pregenomic RNA via a mechanism involving its interaction with 5' stem-loop structure. Virology **2008**; 373:112–23.
37. Ahn SH, Kramvis A, Kawai S, et al. Sequence variation upstream of precore translation initiation codon reduces hepatitis B virus e antigen production. Gastroenterology **2003**; 125:1370–8.

# 肝硬変に出現する血漿アミノ酸不均衡が免疫機構に与える影響

嘉数英二* 上野義之* 下瀬川徹*

索引用語：肝硬変，分岐鎖アミノ酸，栄養免疫

## 1 はじめに

厚生労働省の報告によると平成21年の死亡原因において肝疾患は15,969人，肝臓癌は32,725人と肝臓関連死の割合は極めて高く，これらの患者の大部分に肝硬変が存在する．肝硬変では，糖・蛋白・アミノ酸・脂質・ビタミン・ミネラルなど極めて多岐にわたる栄養代謝障害が出現する．特に血漿中のアミノ酸不均衡に関しては分岐鎖アミノ酸(BCAA)が低下し芳香族アミノ酸(AAA)が増加しFischer比が低下することが古くから知られている[1,2]．進行した肝硬変では肝癌・肝不全だけでなく肺炎・特発性細菌性腹膜炎(SBP)などの感染症が予後を左右する．これは，肝硬変患者は易感染性宿主であり免疫異常が存在することを示唆する．

近年の基礎的な研究報告によるとアミノ酸はただ単に細胞骨格やさまざまな代謝経路の基質となるだけでなく，インスリンとともにmTORを介した栄養感受性シグナル経路に作用し，細胞機能を調節することが解明されてきている[3~5]．さらに，免疫に関してもmTORシグナルが抗原提示細胞の機能に関与することが報告されてきている[6,7]．

本稿では免疫に影響を与える代表的な遊離アミノ酸について過去の文献を基に解説するとともに肝硬変に出現する血漿中アミノ酸不均衡が免疫細胞にいかなる影響を与えるのかを考察する．

## 2 免疫細胞に影響を与える遊離アミノ酸

### 1. グルタミン(L-Glutamine: L-Glu)

非必須アミノ酸であるグルタミンは以前よりリンパ球を含めた細胞増殖に重要であることが知られ[8]，細胞培養の際に培養液に添加される．*In vitro*において細胞外のグルタミン濃度を高めるとT-cellの増殖・IL-2産生，B-cellの形質細胞への分化も亢進する[9]．さらにリンパ球の増殖だけでなく単球やマクロファージの機能にも関与しており，培地

*Eiji KAKAZU et al* : An imbalance of plasma amino acids influences the immune systems in patients with cirrhosis
*東北大学大学院医学系研究科消化器病態学分野［〒980–8575 宮城県仙台市青葉区星陵町 2–1］

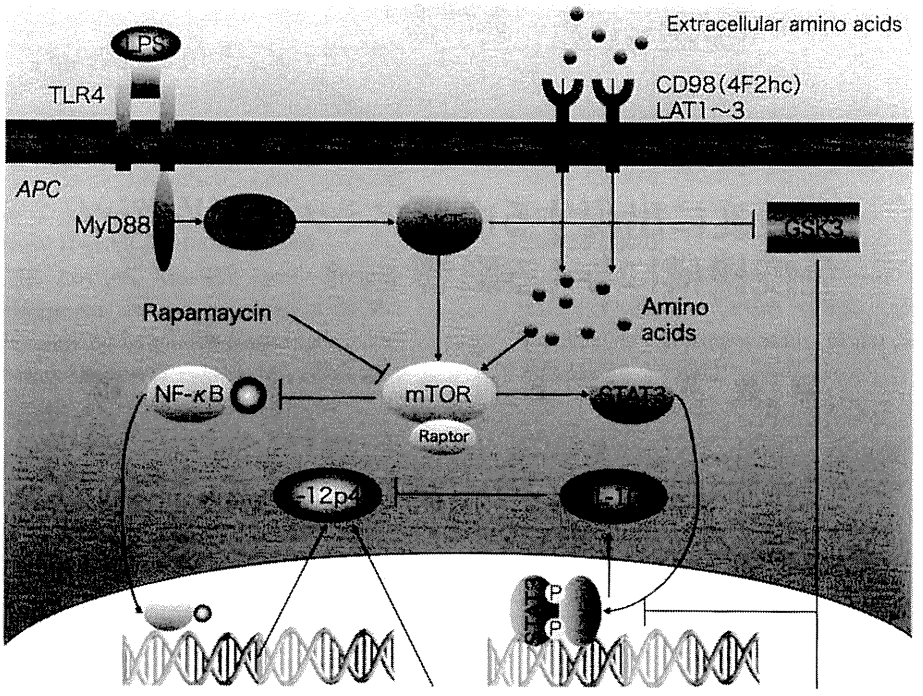


図1　抗原提示細胞におけるmTORシグナルとサイトカイン産生の関係

中のグルタミンの除去により細胞内ATP産生低下に伴う機能低下(MHC class Ⅱ発現低下，貪食能低下，TNF-alpha IL-8の産生低下)が報告されている[9]．最近ではグルタミンとロイシンの双方向性の移動がアミノ酸トランスポーターのSLC7A5/SLC3A2で行われ，mTORシグナルに関与しているとの報告がなされた[10]．肝硬変患者においては，肝硬変の進行とともに血漿中のグルタミン濃度は上昇する傾向がある．これは，肝硬変ではアンモニア代謝のためにL-グルタミン酸→L-グルタミンへの変換が亢進していることによる．

### 2. 分岐鎖アミノ酸(BCAA: L-Valine: L-Val, L-Leucine: L-Leu, L-Isoleucine: L-Ile)

分岐鎖アミノ酸のL-ロイシンがmTORシグナルを調節することが知られ[4,5]盛んに研究が進められている．免疫に関してはmTOR阻害剤であるラパマイシンが樹状細胞のIL-10産生を抑制しIL-12の産生を亢進させ(図1)Th1 / Th2バランスを調節すること[6]，当科では分岐鎖アミノ酸の中でL-バリンが樹状細胞の成熟化に関与していることを近年報告した[11]．分岐鎖アミノ酸の臨床的効果に関しては，肝硬変患者の低下した好中球の貪食能やナチュラルキラー細胞(NK)の活性化が改善されること[12]，さらに樹状細胞機能も改善されること[13]が報告されている．

### 3. トリプトファン(L-Tryptophan: L-Trp)

トリプトファンをキヌレニンに代謝する酵素Indoleamine 2,3-dioxygenase (IDO)はTリンパ球の増殖を抑制し免疫寛容の成立に関与しているとの報告がある[14]．逆に細胞外の過剰なトリプトファン濃度はIDOを介した抑制を阻害することが知られている[15]．東谷らは慢性C型肝炎患者では樹状細胞のIDO活性がLPS+IFN-γ刺激時に亢進しており制御性T細胞の誘導に関与することを報告し

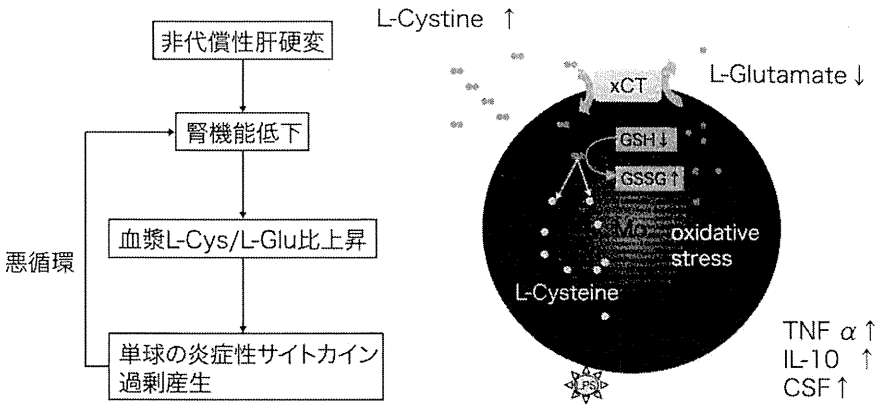


図2　非代償性肝硬変におけるL-シスチン／L-グルタミン酸不均衡が単球に与える影響

た[16]．

### 4. アルギニン(L-Arginine：L-Arg)

アルギニンは腎臓において腸管由来のシトルリンから内因性に産生される非必須アミノ酸である．活性化マクロファージの一酸化窒素(NO)は，誘導型NO合成酵素(iNOS)によりアルギニンから産生され多くの病原体に対する宿主防衛に必須であるので，アルギニンは感染抵抗性の重要な決定因子である[17]．

さらに，アルギニンが枯渇するとTLR4シグナル下流のTPL-2の脱リン酸化が促進しMAPKパスウェイを抑制しTNF-αの産生が抑制されることが知られている[18]．アルギニンが肝硬変患者の免疫に直接与える影響に関しては不明であるが，肝硬変患者，特にSBP患者では腹水中のマクロファージのNOSが亢進していることが古くから知られているため，アルギニンの需要は亢進しているものと考えられる．

### 5. シスチン・グルタミン酸(L-Cystine: L-Cys / L-Glutamate: L-Glu)

古くからL-シスチンとL-グルタミン酸は哺乳類細胞において交換輸送されることが知られていたが，近年その交換輸送体xCTがSato Hらによりクローニングされた[19]．L-シスチンは細胞内に入るとL-システインに還元されグルタチオンの産生に使用される．免疫細胞に関しては，xCTは単球系細胞に発現しているがリンパ球には発現しておらず，さらに抗原提示細胞が放出するL-システインはリンパ球の増殖を調節することが報告されている[20,21]．一方肝硬変患者においては，肝硬変が進行すると血漿中のL-シスチンは増加し，L-グルタミン酸は低下する．特にL-シスチンは腎機能障害が出現すると著明に増加し，LPS刺激を受けた単球からのTNF-αの産生を増加させることが当科の研究で明らかとなった．これらの結果から，L-シスチンが非代償性肝硬変の腎機能に悪循環を与えている可能性を示唆している(図2)．

免疫細胞に作用する代表的な遊離アミノ酸を取りあげたが，他のいくつかのアミノ酸に関しても免疫に作用する報告があり，今後さらなる研究が進められると考える．

## 3 肝硬変で出現するアミノ酸不均衡と免疫へ

肝硬変患者の実際の免疫状態に関しては，血漿中のTNF-alpha, IL-6, IL-1βなどの各種炎症性サイトカインが高いことが古くから

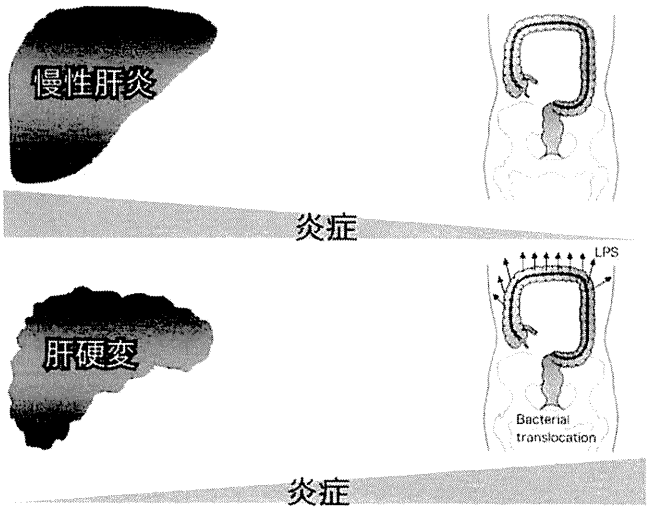


図3　慢性肝炎と肝硬変の炎症場所の違い

表　慢性肝炎・肝硬変患者の血漿中アミノ酸濃度

| | CH (n=33) | Child A (n=81) | Child B (n=57) | Child C (n=35) |
|---|---|---|---|---|
| Glycine | 242 | 216 | 242 | 318 |
| L-Alanine | 393 | 320 | 311 | 368 |
| L-Serine | 130 | 133 | 143 | 178 |
| L-Threonine | 144 | 143 | 149 | 178 |
| L-Cystine | 56 | 60 | 68 | 72 |
| L-Methionine | 31 | 34 | 52 | 70 |
| L-Glutamine | 596 | 607 | 662 | 763 |
| L-Asparagine | 56 | 56 | 64 | 80 |
| L-Glutamic acid | 78 | 66 | 55 | 52 |
| L-Aspartic acid | 4 | 3 | 4 | 5 |
| L-Valine | 247 | 222 | 190 | 184 |
| L-Leucine | 142 | 122 | 107 | 105 |
| L-Isoleucine | 73 | 63 | 56 | 57 |
| L-Phenylalanine | 72 | 78 | 98 | 112 |
| L-Tyrosine | 85 | 98 | 124 | 164 |
| L-Tryptophan | 53 | 50 | 47 | 46 |
| L-Lysine | 222 | 202 | 193 | 198 |
| L-Arginine | 76 | 83 | 88 | 106 |
| L-Histidine | 89 | 83 | 80 | 96 |
| L-Proline | 178 | 156 | 165 | 224 |
| Fischer' s ratio | 3.04 | 2.39 | 1.70 | 1.29 |

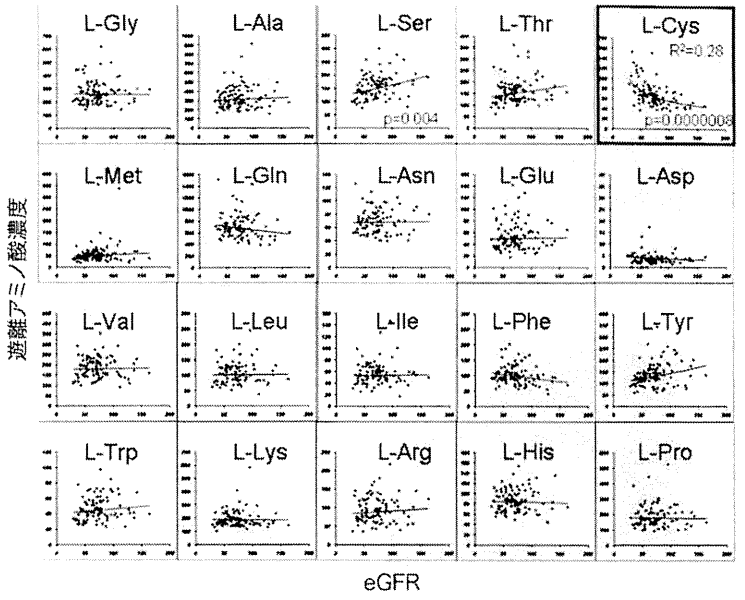


図4　Child-Pugh gradeB orC患者の腎機能と血漿中遊離アミノ酸の関係

知られている[22,23]が，慢性肝炎とは異なり肝硬変では肝臓内での炎症よりもむしろ肝臓外の炎症(細菌感染)による影響を考えなければならない(図3)．マウスを用いた実験では肝硬変では腸管からの細菌刺激(Bacterial translocation)が頻回に起こり，各種免疫細胞の活性状態が持続しているとの報告がある[24～27]．

健常人→慢性肝炎→肝硬変と病状の進行により血漿中のアミノ酸不均衡が出現することは先に述べたが，肝硬変ではChild-Pugh (C-P) grade BやCでその不均衡は著明になる(表)．これは，非代償性肝硬変になると肝臓だけでなく骨格筋や腎臓でのアミノ酸代謝に異常が出現するためである．しかしC-P gradeにはこれらのパラメータは含まれない．C-P grade BまたはCに関して腎機能(eGFR)と各種アミノ酸を比較統計するとC-P gradeではマスクされたアミノ酸異常が明らかとなる(図4)．

これら個々のアミノ酸の変動が免疫に対して良い影響を与えているのか悪影響を与えているのかは依然として不明な点が多いが，BCAAなどの低下しているアミノ酸に関しては，前述のとおり免疫細胞の全アミノ酸需要が亢進していることを考慮すると補充することが良いと考える．一方で増加してくるアミノ酸に関しては，肝硬変の免疫反応に対して悪影響を与えている可能性がある．また，トリプトファンなどの一部のアミノ酸に関しては毒性がいわれており，わずかな変動が免疫に大きな影響を与える可能性がある．

## 4　今後の展開と問題点

肝硬変に出現する血漿中のアミノ酸不均衡が免疫機構へ影響を与えていることは確実である．細胞培養の際にD-MEM, RPMI 1640などの市販されている培地は各種アミノ酸濃度が生体内の濃度よりもはるかに高濃度であるためこの中でアミノ酸の機能解析はできない．さらに，希釈したものを用いたとしても各種アミノ酸は交換輸送されることが多く，

HCM(healthy control medium)
健常人の血漿アミノ酸濃度に一致

ACM(advanced cirrhotic medium)
非代償性肝硬変患者(Child-Pugh grade BまたはC)の血漿アミノ酸濃度に一致

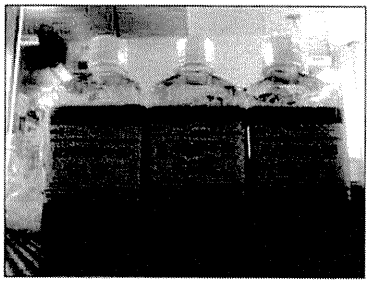

(細胞科学研究所　製造)

| | CCM | HCM | ACM |
|---|---|---|---|
| Glycine | 400 | 225 | 280 |
| L-Alanine | 400 | 391 | 307 |
| L-Serine | 400 | 119 | 151 |
| L-Threonine | 800 | 142 | 138 |
| L-Cystine 2HCl | 200 | 38 | 67 |
| L-Methionine | 200 | 29 | 75 |
| L-Glutamine | 4000 | 564 | 689 |
| L-Asparagine | 400 | 51 | 64 |
| L-Glutamic Acid | 400 | 42 | 53 |
| L-Aspartic Acid | 400 | 3 | 4 |
| L-Valine | 800 | 249 | 175 |
| L-Leucine | 800 | 132 | 100 |
| L-Isoleucine | 800 | 76 | 53 |
| L-Phenylalanine | 400 | 63 | 99 |
| L-Tyrosine | 400 | 65 | 133 |
| L-Tryptophan | 80 | 62 | 45 |
| L-Lysine-HCl | 800 | 183 | 184 |
| L-Arginine-HCl | 400 | 78 | 92 |
| L-Histidine HCl-H2O | 200 | 83 | 85 |
| L-Proline | 400 | 204 | 176 |
| Fischer's ratio | 3.00 | 3.57 | 1.42 |

nmol/mL

*Kakazu E, Ueno Y, et al. Hepatology 2009*

図5　当科で開発したアミノ酸研究用無血清培地

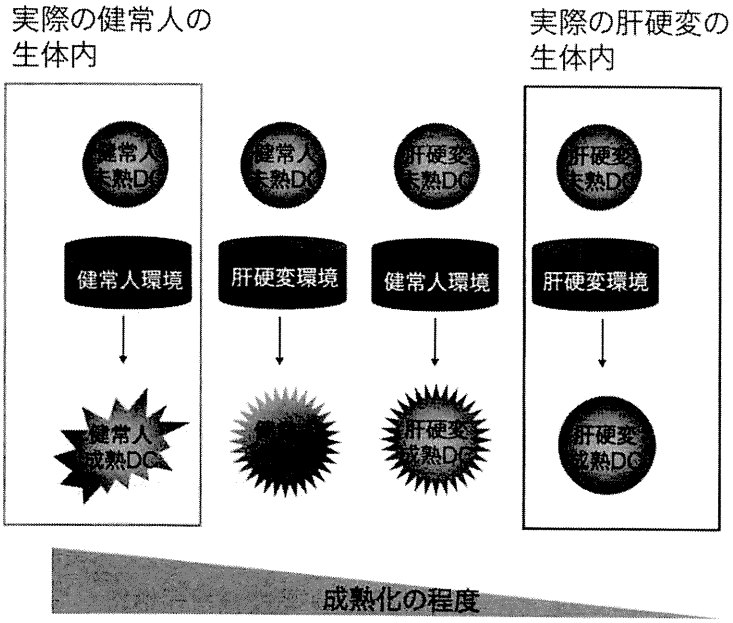


図6　非代償性肝硬変では樹状細胞自体の成熟化が抑制されているだけでなく，血漿中のアミノ酸不均衡が成熟化を抑制する

個々のアミノ酸バランスが重要であるため厳密に生体内の環境を反映しているとはいえない．これらの問題点を解決するために当科では実際の健常人や肝硬変患者の血漿中アミノ酸濃度に一致した無血清培地を開発した(図5)．この培地を用いることで初めて個々のア